

Research of a modified nano-depressure and augmented injection agent

Qianhong Pan ^{1,*}, Yanhong Shen ¹, Xiuhua Liu ¹, Kun Zhao ^{1,2}, Jialu Du ¹, Yali Li ^{1,3}

¹ Xi'an ChangQing Petrochemical Corporation Co.Ltd., Xi'an, 710018, China

² No. 8 Oil Production Factory, Changqing Oilfield Company, CNPC, Xi'an, 716000, China

³ Xi'an Key Laboratory of Tight oil (Shale oil) Development, Xi'an Shiyou University, Xi'an, 710065, China

Abstract. In this paper, the research and application of nanomaterials in oilfield chemical engineering was briefly described with emphasis on the nano-silica in enhanced oil recovery, depressure and augmented injection. A study on the modification of nano-silica was carried out indoors, and a modified nano-depressure and augmented injection agent was prepared by using a coupling agent for surface grafting modification, followed by introducing functional monomers for in-situ modification. The effects of silica dosage, coupling agent dosage, dispersant and regulator ratio, and modification time on the modified product were investigated. It was analyzed by infrared spectroscopy, thermogravimetric analysis, nanoparticle size analyzer, transmission electron microscope, atomic force microscope, etc. A series of experiments were conducted to evaluate the temperature and salt resistance, wettability, as well as depressure and augmented injection performance of the modified products.

Key words: Oilfield chemical engineering; nanosilica modification; enhanced oil recovery; depressure and augmented injection

1. Introduction

Nanomaterials are defined as materials with at least one dimension in the three-dimensional structure ranging from 1 to 100 nm. They have many unique properties such as surface effects, volume effects, quantum size effects, macroscopic quantum tunneling effects, and mechanical properties effects. In oilfield chemical engineering, it mainly involves nanomaterials in many different forms, including nanoparticles, nanofilms, nanocrystals, nanofibers, and nanofluids. In drilling and completion construction, as a kind of additive, nanomaterials play a great role in reducing the liquid filter loss, enhancing the walled performance of drilling fluid, improving the pore structure of cementing cement ring and the construction quality. After adding nanomaterials to the drilling fluid, it was found that its lubrication was improved and the construction friction was significantly reduced. In addition, the rheology, lubrication, mud cake wall-building and crack sealing properties of drilling fluid were greatly improved, while the pore penetration of cement ring and the thickening time of the cement slurry were reduced. The introduction of nanomaterials in the fracturing fluid system can improve its rheology and sand suspension, form a more quality crack network system, enhance the fracturing construction effect, and improve the efficiency of increasing production and transformation.[1-4] It can meet the current effective

development of low permeability reservoirs and unconventional oil and gas. The application of nanomaterials in oil recovery has become a research topic, especially in the nanomaterials to change rock wettability, reduce the oil-water interface tension, flood oil, pressure depressure and augmented injection. With a large number of unsaturated functional groups on their surface, nanomaterials can efficiently catalyze the organics and bacteria in oilfield sewage so as to make the emulsification separation of oil and water through oil absorption and demulsification. In addition, the integral aerogel material can be constructed based on the structural unit of nanomaterials, and the dual function of demulsification and oil-water separation can be realized.[5-10]

The conventional resistance reduction, depressure and augmented injection measures adopted in the low permeability oilfield are mainly divided into two categories: reservoir modification and rock surface modification. Among them, the reservoir modification mainly includes fracturing and acidification technology. Rock surface modification uses surfactant to form an adsorption layer on the pore surface of the oil layer, which increases the injection by reducing the interface tension of solid and liquid. Field tests also show that fracturing can cause the formation flow, water rush, causing irreversible damage to the formation, and the short validity period of acidification can easily cause cumulative damage and

* Corresponding author: 314505704@qq.com

pollution to the formation. The adsorption force of surfactant on the rock surface is weak and short, and its application effect is also greatly limited.[11-14]

In recent years, more and more researchers pay attention to nano depressure and augmented injection technology, its technology is to bring nanoparticles into the reservoir through specific dispersion, and adsorb and deposit in the appropriate position, change the wettability and roughness of the micropore wall, form the surface microstructure, so that the micropore wall produces a large sliding length, thus playing the purpose of depressure and augmented injection. Needle from oil field water injection process field, this paper proposed a kind of modified nanomaterials with a water phase system for depressure and augmented injection. The silica dosage, coupling agent dosage, dispersant and regulator ratio, and modification time on the modified product were investigated, and the optimum synthesis method and parameters were determined.

2. Materials and methods

2.1 Materials

Materials used for the study such as ethanol (Sinopharm Co., Ltd.), hydrochloric acid (Tianjin Damao Chemical Co., Ltd.), coupling agent (Nanjing New Materials Co., Ltd.), silica (Shanghai Kay Chemicals Co., Ltd.), functional monomer (Shanghai Kay Chemicals Co., Ltd.) were purchased, respectively. Dispersants, stabilizers were synthesized in the laboratory.

The resulting modified silica was characterized by Fourier Transform Infrared Spectrometer (Nicolet Summit, Thermo Fisher Scientific Co., Ltd., USA); TGA-DSC thermal analyzer (TG-SDTA851, Mettler-Toledo Co., Ltd., Switzerland); laser particle size distribution analyzer (NANO ZS90, Malvern Instruments Co., Ltd., UK); transmission electron microscope (HT7800, Hitachi Co., Ltd., Japan); atomic force microscope (SPM-9700HT, Shimadzu Co., Ltd., Japan); scanning electron microscope (Nova NANOSEM450, FEI Co., Ltd., USA); contact angle measuring instrument (DSA30, Clues Co., Ltd., Germany). The HA-2 integrated oil flooding device was used to evaluate the depressure and augmented injection performance through the core flow experiment. The properties of anti-calcium sulfate scale and anti-swelling percentage were evaluated according to the formulas in Standard Q/SY 126 and SY/T 5971.[15-19]

2.2 Preparation of nanosilica

A certain amount of nanosilica was slowly added to the dispersant and stirred at a certain temperature to form solution 1. In addition, the coupling agent and the modifier were added to a certain amount of the regulator, and the solution 2 was formed by stirring at 25 °C, and then the solution 2 was slowly added to the solution 1. The reaction was carried out at a certain temperature for 6 h to obtain a modified nano-depressure and augmented injection agent with water-phase system.

3. Results and discussion

3.1 Nanosilica selection and dosage determination

The solid content of the nanosilica was determined using the standard GB 12005.2. A certain amount of nanosilica was added to the dispersant to form a uniform liquid, and then its particle size was determined to gradually increase the amount of nanosilica until the particle size was greater than 100 nm.

Table.1 Solid content of nanosilica

Order number	Sample number	Appearance	Solid content (%)
1	1#	White emulsion	22
2	2#	White emulsion	62
3	3#	White emulsion	57
4	4#	Conviscous homogeneous liquid	8
5	5#	Conviscous homogeneous liquid	20
6	6#	White powder	98
7	7#	Homogeneous liquid	48

Table.2 Determination of the dosage of nanosilica

Order number	Sample number	Nanosilica dosage (%)			
		4	8	16	32
		Particle size corresponding to the dosage of nanosilica (nm)			
1	1#	231	323	434	567
2	2#	121	145	156	189
3	3#	168	201	218	248
4	4#	136	219	232	276
5	5#	120	160	204	289
6	6#	130	143	156	183
7	7#	32	31	36	87

As shown in from Table 1 and Table 2, it can be found that the particle size began to increase when the dosage of nanosilica was 32%. Therefore, the orthogonal trials were designed with the dosage of nanosilica of 4%, 8%, 16%, and 32%.

3.2 Determination of the dosage of the coupling agent

When the dosage of nanosilica was 16%, the reaction time was 4 h and the temperature was 60 °C, and the effect of the coupling agent dosage on the grafting percent was explored to determine the selection range of orthogonal trials. According to Table 3, the grafting percent of nanosilica was maximum at the coupling agent dosage of 0.8%. When the coupling content was further increased, the grafting percent decreased slightly, due to the large amount of the coupling agent hydrolysis will partially self-polymerization, enhanced competitive reaction, and decreased grafting percent. Therefore, in the orthogonal trials, the dosage of the coupling agent was determined as 0.1%, 0.2%, 0.4% and 0.8%.

Table.3 Determination of the range of coupling agent dosage

Order number	Coupling agent dosage (%)	Grafting percent
1	0.1	0.0476
2	0.2	0.0521
3	0.4	0.0618
4	0.8	0.0763
5	2	0.0431
6	4	0.0354
7	8	0.0321
8	10	0.0336

3.3 Modifier selection and dosage determination

The performance of functional monomers was evaluated using standard Q / SY 126 and the experimental results are shown in Table 4.

Table.4 Selection of modifiers

Order number	Sample number	CaCO ₃ prevention percent (%)	CaSO ₄ prevention percent (%)	BaSO ₄ prevention percent (%)
1	1#	63.71	4.91	40.63
2	2#	86.69	98.75	2.74
3	3#	83.87	9.72	0
4	4#	87.90	98.33	/
5	5#	43.95	78.89	8.21
6	6#	/	0.52	/
7	7#	59.27	31.87	0.1
8	8#	70.65	96.67	1.16
9	9#	70.44	87.29	2.21
10	10#	59.96	97.71	38.32
11	11#	73.79	97.92	4.84
12	12#	83.44	0	0

Based on the results of Table 4, and according to its functional group structure, and the comprehensive performance, it is determined to use 2# as the optimal modifier. When the dosage of nanosilica was 16%, the reaction time was 4 h and the temperature was 60 °C, and the effect of the ratio of dispersant and modifier on the grafting percent was explored to determine the selection range of orthogonal trials. As shown from Table 5, the ratio of dispersant and modifier was 4:1, the grafting percent of nanosilica was maximum. Subsequently, the graft percent decreased when the ratio of dispersant and modifier increased. Therefore, in the orthogonal trials, the ratio of dispersant and modifier was 1:1, 2:1, 3:1 and 4:1.

Table.5 Determination of the ratio of dispersant and modifier

Order number	The ratio of dispersant and modifier	Grafting percent
1	1: 1	0.0234
2	2: 1	0.0317
3	3: 1	0.0402
4	4: 1	0.0533
5	5: 1	0.0421
6	6: 1	0.0414
7	7: 1	0.0401

3.4 Investigation of the optimal modification condition

Orthogonal trials with the four factors and four level were designed so as to investigate the effect of nanosilica dosage (factor A), coupling dosage (factor B), the ratio of dispersant and modifier (factor C), reaction time (factor D) on the particle size of nanosilica, as shown in Table 6.

Table.6 Orthogonal table

Level	Experimental factor			
	Nanosilica dosage (%)	Coupling agent dosage (%)	The ratio of dispersant and modifier	reaction time (h)
	Factor A	Factor B	Factor C	Factor D
1	4	0.1	1: 1	2
2	8	0.2	2: 1	4
3	16	0.4	3: 1	6
4	32	0.8	4: 1	8

Table.7 Orthogonal scheme and the structural intuitive analysis

Order number	Experimental factor					the particle size (nm)
	Nanosilica dosage (%)	Coupling agent dosage (%)	The ratio of dispersant and modifier	reaction time (h)		
	Factor A	Factor B	Factor C	Factor D		
1	1 (4)	1 (0.1)	1 (1: 1)	1 (2)		1419
2	1 (4)	2 (0.2)	2 (2: 1)	2 (4)		1233
3	1 (4)	3 (0.4)	3 (3: 1)	3 (6)		667
4	1 (4)	4 (0.8)	4 (4: 1)	4 (8)		774
5	2 (8)	1 (0.1)	2 (2: 1)	3 (6)		877
6	2 (8)	2 (0.2)	1 (1: 1)	4 (8)		642
7	2 (8)	3 (0.4)	4 (4: 1)	1 (2)		585
8	2 (8)	4 (0.8)	3 (3: 1)	2 (4)		108
9	3 (16)	1 (0.1)	3 (3: 1)	4 (8)		270
10	3 (16)	2 (0.2)	4 (4: 1)	3 (6)		416
11	3 (16)	3 (0.4)	1 (1: 1)	2 (4)		342
12	3 (16)	4 (0.8)	2 (2: 1)	1 (2)		523
13	4 (32)	1 (0.1)	4 (4: 1)	2 (4)		85
14	4 (32)	2 (0.2)	3 (3: 1)	1 (2)		226
15	4 (32)	3 (0.4)	2 (2: 1)	4 (8)		63
16	4 (32)	4 (0.8)	1 (1: 1)	3 (6)		68
Level K ₁	4093	2651	2471	2753		
Level K ₂	2212	2517	2696	1768		
Level K ₃	1551	1657	1271	2028		
Level K ₄	442	1473	1860	1749		
k ₁	1023	663	618	688		
k ₂	553	629	674	442		
k ₃	388	414	318	507		
k ₄	111	368	465	437		
R	913	295	356	251		

As shown in Table 7, it was found that the minimum particle size was 63 nm and the optimal combination was selected as A₄B₄C₃D₃. Depending on the magnitude of the

error, the importance of each factor to the particle size of modified nanomaterials can be judged, the dosage of nanosilica (A)> the ratio of dispersant and modifier (C)> the dosage of coupling agent (B)> reaction time (D).

3.5 Performance evaluation of nanosilica

3.5.1 Characterization of nanosilica

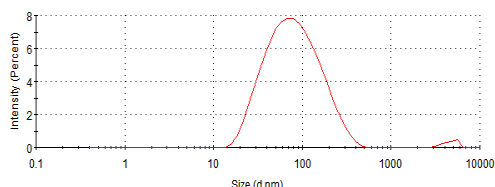


Fig. 1 Particle size of modified nanosilica

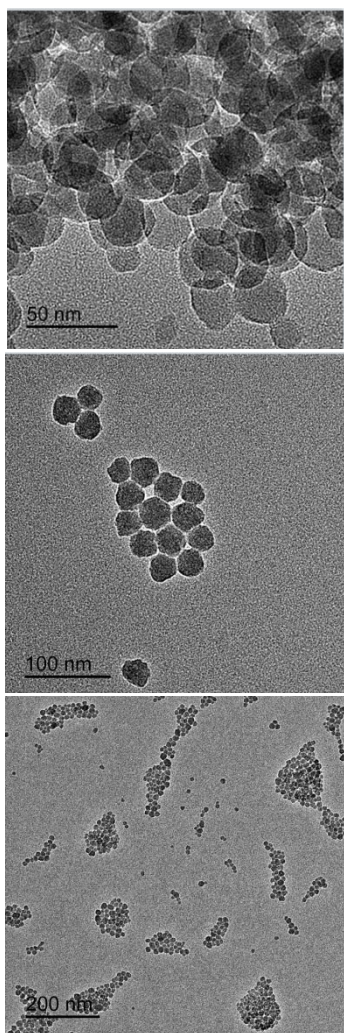


Fig. 2 TEM of modified nanosilica

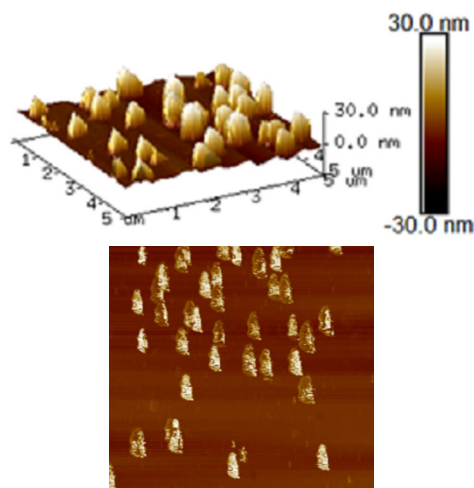


Fig. 3 AFM of modified nanosilica

As shown in Fig. 1, Fig. 2 and Fig. 3, it is clear that the particle size of the modified nanomaterials is less than 100 nm.

3.5.2 Determination of salt resistance

Modified nanosilica was added to 40 g/L salt solution at 60 °C in comparison with conventional modified nanosilica and unmodified silica, and the salt resistance result was shown in Fig. 4. It can be found that the modified nanosilica has a high salt resistance ability.

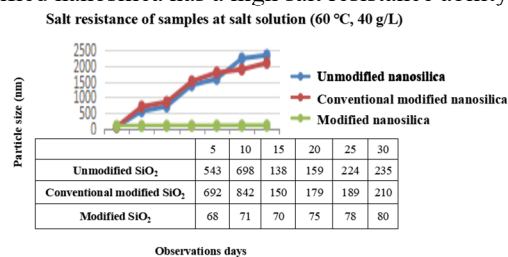


Fig.4 Salt resistance of modified nanosilica

3.5.3 Functional evaluation

The evaluation results of anti-scale and anti-swelling performance were shown in Table 8 and Table 9. It can be found that the modified nanosilica enhance the prevention percent and anti-swelling percentage obviously.

Table.8 Anti-scale performance of modified nanosilica

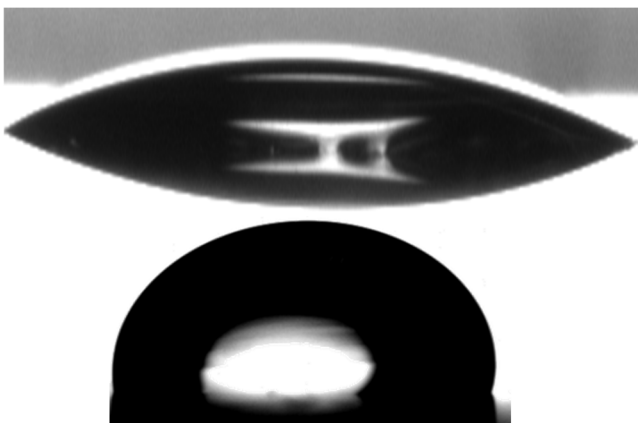
Sample number	CaCO ₃ prevention percent % (100 mg/L)	CaSO ₄ prevention percent % (100 mg/L)	BaSO ₄ prevention percent % (100 mg/L)
Unmodified nanosilica	1.2	1.6	0
Conventional modified nanosilica	0.3	0.5	0
Modified nanosilica	68	98	10

Table.9 Anti-swelling performance of modified nanosilica

Sample number	Anti-swelling percentage % (0.5%)
Unmodified nanosilica	3.5
Conventional modified nanosilica	2.7
Modified nanosilica	14

3.5.4 Evaluation of wettability

With 40 g/L salt solution as solvent, a certain amount of 0.5% sample solution was prepared. The slide was immersed in the sample solution for 4 h, and then removed and dried, measuring the wettability of distilled water on its surface, as shown in Fig. 6(a-b). The contact angle of Fig. 6(a) was determined as 10°, indicating its hydrophily after the immersion of the unmodified nanosilica solution. The contact angle of Fig. 6(b) was determined as 102°, indicating its hydrophobicity after the immersion of the modified nanosilica solution.



(a) Unmodified nanosilica (b) Modified nanosilica

Fig. 6 Contact angles of unmodified nanosilica and modified nanosilica

3.5.5 Performance evaluation of depressure and augmented injection

Take a cleaned core and measure the air permeability. The saturated salt solution was then loaded into the displacement device as shown in the Fig. 10, and a certain “PV” was continuously displaced with salt solution at a certain flow rate “Q” to ensure that the system was stable, and then record the pressure difference “ΔP₀” before and after. Change the flow rate “Q”, record the pressure difference before and after and calculate the permeability “K_{0W}”. In the constant current mode, a modified nanosilica agent was used for displacement, and the pressure difference “ΔP₁” before and after was recorded, and different flow rates “Q” were changed, the pressure difference before and after was recorded, and the phase permeability “K_{0Y}” was calculated. After the modified nanosilica was displaced to a certain “PV”, it is replaced by salt solution, and the pressure difference “ΔP₂” before

and after. Change the flow rate “Q”, record the pressure difference before and after and calculate the permeability “K_{0Z}”. The following formula to calculate the depressurization rate (A) and the change of permeability (K).[20-23]

$$A = \frac{\Delta P_0 - \Delta P_2}{\Delta P_0} \times 100\%$$

$$K = \frac{\Delta K_0 - \Delta K_{0Z}}{\Delta K_0} \times 100\%$$

Three cores were collected to determine the depressure and augmented injection performance of the modified nanosilica. The evaluation results were as follows. The Table10 showed that the modified nanosilica had a considerable depressure effect.

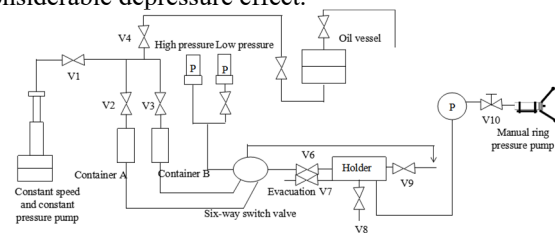


Fig. 7 Flow chart of the depressure and augmented injection and displacement device

Table.10 Performance of of depressure and augmented injection based on modified nanosilica

Core number	Core air permeability(mD)	Reduced pressure rate% (0.5%)	Rate of change in permeability % (0.5%)	Sample name
1#	3.2	-0.6	-12.3	Unmodified nanosilica
2#	4.1	1.4	0.1	Conventional modified nanosilica
3#	3.8	13	2.45	Modified nanosilica

4. Conclusions

The development of nanofluids in hypotonic and extreme low permeability reservoirs has a broad development prospect, which can be in the direction of simple process, controllable synthetic structure and long-term stable dispersion. In this paper, a modified nanomaterials were prepared by coupling agent grafting modification and surface modification technology. When the reaction temperature was 60 °C, the modification time was 6 h, the amount of nanosilica was 16%, the coupling agent was 0.8%, and the ratio of dispersant and modifier was 3:1, the particle size of the modified nanosilica is 63 nm, and the optimal modification effect was achieved. Indoor

displacement experiment showed that it has a considerable effect of depressure and augmented injection.

References

1. Cui CH, Li XJ, Zhang YZ, et al. Application of novel surfactant system with low content in low permeability reservoir[J]. *Advances in Fine Petrochemicals*, 2004, 5(1): 7-9.
2. Liu K. The effect of cationic and zwitterionic surfactants[J]. *Journal of Petrochemical Universities*, 2013, 26(5): 55-59.
3. Ma HY, Pan Y, Yang SC. Study on determining methods of anionic surfactants[J]. *Contemporary Chemical Industry*, 2013, 42(3): 373-375.
4. Wang H, Ren XJ, Li DY, et al. Experimental research on decreasing injection pressure with surfactant in Langdong oil field[J]. *Liaoning Chemical Industry*, 2010, 39(10): 1007-1009.
5. Fang XH. The behaviors of several kinds of surfactant system and effects on decreasing displacement pressure[J]. *Petroleum Geology & Oilfield Development in Daqing*, 2002, 21(2): 62-63.
6. Tang JZ, Fang XH. Research and application of decreasing injection pressure by surfactant in low permeability reservoir[J]. *Chemical Industry Times*, 2004, 18(1): 51-54.
7. Qu JK, Zhu YY, Zhou GY. Application of efficiency and effectiveness on surfactants flooding system[J]. *Science & Technology in Chemical Industry*, 2004, 12(1): 1-4.
8. Yang Y, Liu YB, Pu WF, et al. The research progression and prospect of a new generation of Gemini surfactants[J]. *Petroleum Geology and Recovery Efficiency*, 2005, 12(6): 67-70.
9. Tan ZL, Han D, Yang PH. The properties and application prospect in enhanced oil recovery of Gemini surfactants[J]. *Oilfield Chemistry*, 2003, 20(2): 187-191.
10. Wu YH, Gong H, Xia KJ, et al. Applicability of a nano-silica microemulsion for depressurization and injection of low permeability reservoirs[J]. *Drilling & Production Technology*, 2020, 43(2): 111-114.
11. Guo Y. Discussion on the technical difficulties and development countermeasures of low-permeability oilfield exploitation[J]. *Chemical Industry Management*, 2017 (24): 121.
12. Shu SL, Guo YC. Study and application of seepage mechanism of special low-permeability reservoir[J]. *Oil and gas geology and recovery*, 2016, 23(5): 58-64.
13. Qu ZQ, Qi N, Wang ZQ, et al. New progress in acidification transformation of low permeability oil layer[J]. *Oil and gas geology and recovery rate*, 2006, 6: 93-96.
14. Yin Y, Jia JF. An anionic complex microemulsion system is preferred and effective fruit[J]. *Applied chemical industry*, 2018, 47 (6): 1105-1108.
15. Gao M, Song KP. New sulfobetaine suitable for low permeable sandstone oil layer surfactant studies[J]. *Oilfield chemistry*, 2008, 3: 265-267.
16. Feng AZ, Zhang JQ, Jiang P, et al. Experimental study of depressurization and augmented injection by high concentration surfactant system for low permeability reservoir[J]. *Oilfield Chemistry*, 2011, 28(1): 69-73.
17. Zhang J, Zhang G, Ge J, et al. Laboratory studies of depressurization with a high concentration of surfactant in low-permeability reservoirs[J]. *Journal of Dispersion Science & Technology*, 2012, 33(11): 1589-1595.
18. Zhang X, Liu D, Li L, et al. Synergistic effects of surfactants on depressurization and augmented injection in high salinity low-permeability reservoirs: formula development and mechanism study[J]. *Colloids and Surfaces A: Physicochemical and Engineering Aspects*, 2021.
19. Xiong S, Shi L, Cheng S. Study of depressure and augmented injection agents for low permeability oilfields[J]. *Journal of Petrochemical Universities*, 2014.
20. Chen G, Lai N. Study on the adaptability of depressurization and injection of MD film in low permeability reservoirs[J]. *IOP Conference Series: Earth and Environmental Science*, 2019.
21. Hua Y, Li F, Li W. Decompression and augmented injection theories research of nanometer polysilicon in oilfield water flood development[J]. *Natural Science Journal of Harbin Normal University*, 2005.
22. Wang K, Wang C, Sun L, et al. Experimental research on decompression and augmented injection effect by using active SiO₂ nano-powder in middle and low permeability cores[J]. *IEEE*, 2010:1-4.
23. Zhang X, Liu D, Li L, et al. Synergistic effects of surfactants on depressurization and augmented injection in high salinity low-permeability reservoirs: formula development and mechanism study[J]. *Colloids and Surfaces A: Physicochemical and Engineering Aspects*, 2021.